RSC Advances

PAPER

View Article Online
View Journal | View Issue

Check for updates

Cite this: *RSC Adv.*, 2021, **11**, 27978

Synchronizing chemistry, quantum mechanics and radioactivity in a revolutionary renewed atom model. Part 1: the elements where *Z* is 1–10 (H, He, Li, Be, B, C, N, O, F, Ne)

Gerard W. M. Visser and Albert D. Windhorst *

Received 6th May 2021
Accepted 30th July 2021

DOI: 10.1039/d1ra03529k

rsc.li/rsc-advances

The alliance between the reigning quantum mechanical atom model and chemistry still is a difficult one when it comes to an adequate explanation for *e.g.* the covalent bond, inversion, chirality, or hydrogen bonds. Overruling Rutherford's extrapolation from gold to hydrogen, an atom model is described that provides improved answers to these phenomena while the hybridization principle and the covalent bond are re-defined by giving neutrons a much more prominent role than they have in the reigning quantum mechanical model. It is postulated that a neutron is not just there to assist the strong force in surpassing the repulsive coulombic forces between the protons in the nucleus, but the neutron is the modus operandi of molecular geometry, and as such plays a part in chemical reactivity, bond length and bond strength.

Open Access Article. Published on 19 August 2021. Downloaded on 2/7/2026 11:39:10 PM.
This article is licensed under a Creative Commons Attribution-NonCommercial 3.0 Unported Licence.

1 Introduction

Based on the experience that an atom contains positive and negative charges, Thomson was the first to design a model of the atom (1904).[1,2] The positive charge formed a ball of even density, with the negatively charged electrons floating in the ball and forming regular geometric patterns by mutual repulsion. From the famous experiment (bombarding thin gold foils with alpha particles) performed by his students, Rutherford concluded in 1911 that Thompson's model required a serious adjustment: the complete positive charge and almost the entire mass of an atom are concentrated in a very small volume, the dense inner core of an atom, the nucleus.[3] This solar system model (electrons revolving in circular or elliptical orbits around the nucleus like planets around the sun) evolved *via* Bohr[4] and Schrodinger/Heisenberg[5,6] into the quantum mechanical atom model of today. This means a model with orbitals/probability clouds (areas within which an electron can be encountered) instead of orbits of an electron, and with neutrons plus protons bound together by the so-called strong force in the nucleus, accounting for 99.9% of the atom's mass. This strong force surpasses the Coulomb repulsion between the protons; if not, the nucleus of the atom converts to an energetically better situation by radioactive decay. In the latter case, the so-called weak nuclear force plays a role.

With respect to chemical aspects, the octet rule (1916) had been implemented as the closed shell principle, the "Aufbau principle" had seen the light, and Pauling[7] had developed the hybridization concept (sp^3 for single-bonded carbon, sp^2 for double-bonded carbon, sp^1 for triple-bonded carbon) as a proposition to account for the otherwise inexplicable fact that *e.g.* CH_4 contains four equal CH-bonds. This hybridization concept also solved the issue of how a p-electron crosses a node and passes through the positively charged nucleus. A covalent bond became the result of overlap between two orbitals (two interfering waves, each with one electron) and two paired electrons, inversion (*e.g.* the NH_3 molecule) and hydrogen bonds became the result of spontaneous tunneling.[8,9] Even empty orbitals could exhibit chemical reactivity such as the empty p-orbital of boron and alumina, and empty d-orbitals in case of octet rule disobeying compounds like H_3PO_4, H_2SO_4 or $HClO_4$. The octet rule disobeying HNO_3 remained a nuisance, because nitrogen's quantum number $n = 2$ forbids the presence of d-orbitals; only a Lewis structure remained descriptive for this compound.[10]

At around the time Ogilvie questioned the whole orbital concept,[11] we added an extra dimension to Pauling's geometric s-electron hybridization parameter. Organic fluorine chemistry is rather unusual and numerous dichotomies exist.[12] Some of these are accounted for by hypotheses like 'double-bond no-bond resonance'[13] or 'large repulsion integrals in the carbon-fluorine region'.[14] In an attempt to improve on this, we launched the concept of the s-orbital density deficiency of the F-atom as the driving force of its chemical behavior.[15–17] This concept was based on the quantum mechanical fact that lone pairs require more than their s-share in the sp^3-hybridization process.[18] Since F possesses three lone pairs, we postulated (1) that the F-atom is urgently in need for additional s-orbital

Amsterdam UMC, Vrije Universiteit Amsterdam, Dept. Radiology & Nuclear Medicine, De Boelelaan 1117, 1081HV Amsterdam, The Netherlands. E-mail: ad.windhorst@amsterdamumc.nl

© 2021 The Author(s). Published by the Royal Society of Chemistry

Open Access Article. Published on 19 August 2021. Downloaded on 2/7/2026 11:39:10 PM.
This article is licensed under a Creative Commons Attribution-NonCommercial 3.0 Unported Licence.

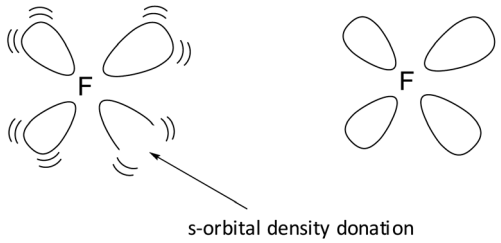

Fig. 1 Principle of s-orbital density deficiency and s-orbital density donation.

density *via* its bonding orbital, to release this tension (see Fig. 1), and (2) that the hydrogen atom and the carbon atom are the perfect s-orbital density donors for the F-atom.

According to this concept, the F-atom in F_2 is the most s-orbital density deficient, leading to a weak F–F bond and extreme reactivity; in CH_3COOF this situation is slightly better and therefore it reacts less vigorous. Over and above that, although being the most electronegative element in the periodic system, when present as fluoride in water, the F-atom immediately shares its extra electron to form HF in exchange for s-orbital density, whereas fluoride is a strong nucleophile in the absence of H_2O. The concept also made clear why in organic chemistry the F-atom prefers to be bound to sp^3-carbon over sp^2-carbon: the sp^2-carbon atom had to use a great deal of its s-orbital density to construct the double bond and, therefore, its s-orbital density donor ability towards fluorine is diminished.

Later on, we reported that in a series of mono-substituted benzyl analogues of thioperamide, the aromatic F-derivatives showed, in contrast to computer predictions, a factor 10 less *in vitro* activity than its H, Cl, Br, and I counterparts (Fig. 2).[19]

We postulated that the aromatic ring of the fluor derivative was not flat anymore,[20] because F had forced the sp^2-carbon of the aromatic ring to re-hybridize into a sp^3-like carbon, leading to a Dewar benzene-like structure with reduced affinity for the receptor. In addition, we argued that also for fluorobenzene itself the literature data[21] (*ipso* angle increase and apparent bond shortening plus angle decrease for C_2 and C_3) strongly point to a non-flat configuration (Fig. 3 and 4).

The last decennia we have tried to find an adequate explanation for the re-hybridization phenomenon. We gradually came to the inevitable conclusion that the reigning atom model

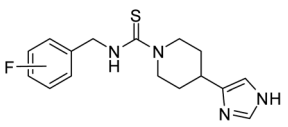

R	pA_2 (±SEM)
H	7.32 (0.16)
2-F	6.04 (0.14)
3-F	6.44 (0.13)
4-F	6.25 (0.14)

Fig. 2 Fluorobenzyl thioperamide derivative, remarkably deviating a factor 10.

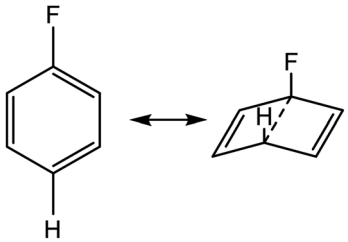

Fig. 3 Fluorobenzene transforming into fluor Dewar benzene.

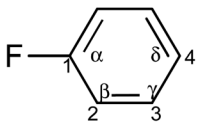

	Bond length (Å)	Angle	
C_1 - F	1.356	α	123.4°
$C_1 - C_2$	1.387	β	118.0°
$C_2 - C_3$	1.399	γ	120.2°
$C_3 - C_4$	1.401	δ	120.2°

Fig. 4 Apparent bond shortening and angle changes when projected in flat fluorobenzene (angles and bond lengths are from [21]).

needed adjustment, and hereto some serious 'out of the box thinking' was required. Besides finding a concrete answer to the fluorine problem, it would be an added bonus when at the same time this renewed atom model would also comprise an adequate solution for phenomena like inversion, chirality and hydrogen bonds, and the reason for stability and instability of an atom. In this paper we report our proposal for such an atom model adjustment. The renewed atom model is based on the key premise that Rutherford's extrapolation of the findings for the heavy gold atom ($Z = 79$) to the lighter atoms, is not correct.

2 The new model

2.1 Central thesis and definitions

In this part 1 paper we discuss our proposition for the atom configuration of the elements with $Z = 1$–10. We will just stick to the level of protons and neutrons held together by the strong force *via* quarks. Production and decay of their radioactive isotopes are used as confirmation of the proposed atom structure.

The new model will be discussed along the following lines:

2.1.1 Central thesis. (1) The nucleus of atoms with low Z is not a dense, concentrated bunch of neutrons and protons in some inner core, but a flexible constellation of neutrons and protons that can rock, stretch and bend (Fig. 5).

(2) This flexible constellation of neutrons and protons is strictly organized. Two protons are always separated from each other by a neutron; two neutrons are always separated from each other by a proton.

(3) In each constellation a neutron can bind to three protons at most, a proton can bind to three neutrons at most, because each have three strong force related quarks.

Open Access Article. Published on 19 August 2021. Downloaded on 2/7/2026 11:39:10 PM.
This article is licensed under a Creative Commons Attribution-NonCommercial 3.0 Unported Licence.

Fig. 5 (Left) Rocking, stretching and bending of the $^4_2$He-atom. (Right) In the $^4_2$He-unit, the anchor protons together form the anchor proton side and will be drawn on the low side throughout the paper; the anchor neutrons together form the anchor neutron side and are always drawn on top.

(4) In the strictly organized constellation of neutrons and protons each electron remains revolving in a probability cloud around its proton.

(5) A "square" proton or "square" neutron can be part of the strictly organized constellation of neutrons and protons. A square proton is defined as a proton that carries an electron that is too low in energy to chemically bind to another atom and therefore needs to become activated by a neutron (hybridization); a square neutron is defined as a neutron that is too low in energy to activate a square proton or to take part in hybridization.

2.1.2 Building block and subunits. For the elements Li ($Z = 3$) through Ne ($Z = 10$) the basic building block is a $^4_2$He-unit. Throughout the paper, the two neutrons of the $^4_2$He-unit will be called the anchor neutron side and will be drawn on top; the two protons of the $^4_2$He-unit will be called the anchor proton side and will be drawn on the low side (Fig. 5). Subunits at the anchor neutron side will bear the subscript N, subunits at the anchor proton side subscript P.

Nomenclature used for the subunits at the basic building block:

(a) P_N is a proton at the anchor neutron side of the basic building block; N_P is a neutron at the anchor proton side;

(b) D_N is a subunit consisting of a neutron and a proton at the anchor neutron side; D_P is the same subunit at the anchor proton side;

(c) T_P is a subunit consisting of two neutrons and a proton at the anchor proton side; a T_N subunit is only present in extremely short-living radioisotopes.

(d) $^3_2He_N$, $^4_2He_N$, $^4_2He_P$ and $^5_2He_P$ are subunits consisting of two protons and one, two or three neutrons, respectively, at the anchor (N or P) sides, and correspond chemically with a lone pair and quantum mechanically with a filled subshell; $^3_2He_P$ and $^5_2He_N$ are only present in extremely short-living radioisotopes.

(e) The * in subunits D^*_N, T^*_P, $^4_2He^*_N$ and $^5_2He^*_P$ indicate that they bear a square neutron; P_N and $^3_2He_N$ nearly always bear a square proton.

(f) A covalent bond implies formation of a "chemical" helium-unit between a P_N, D_N, D_P or T_P subunit of one atom and one of the subunits of the other atom.

(g) In the figures, the neutrons are depicted yellow, the protons blue; square neutrons are depicted as yellow stars, square protons as blue stars; in unstable atoms, neutrons are depicted pink, protons red. For the sake of clarity, in atoms $Z =$ 5 and higher, the anchor neutrons of the basic building $^4_2$He-block are depicted white, the anchor protons dark grey.

2.1.3 Radioisotopes, production and decay. – Production and decay of radioactive isotopes are used as confirmation. To this end, all isotopes and radioisotopes are written as ^A_ZX wherein mass number A represents the number of protons plus neutrons, atomic number Z the number of protons, and X the element.

– A nuclear reaction is denoted as X (a, b) Y wherein X is the target element, a is the incoming particle, b is the outgoing particle and Y the newborn isotope; as a consequence of the impact, radioisotopes produced in a cyclotron or neutron generator do not contain square protons or square neutrons.

– Because in the new model every proton is separated by a neutron and *visa versa* (thesis 2, *vide supra*), the newborn proton formed after β^--decay requires a shift within the constellation of the atom (away from the proton to which the disintegrated neutron was attached). The newborn neutron formed after β^+-decay needs a likewise transfer (away from the neutron to which the disintegrated proton was attached).

– An isomeric transition (IT) is a transfer of a neutron within the constellation of the atom to an energetically more favorable position (often temporarily better).

– Electron capture (EC) implies a transfer of the newborn neutron away from the neutron to which the proton was attached before capturing its electron.

Most of the production routes and decay modes can be found in the book Radionuclide Transformations.[22] Because individual referring to physicists involved in accurate determination of half-lives and isotope abundancies would make the reference list extremely long, we would like to thank them warmly here.

2.2 The new model at work: the carbon atom ($Z = 6$)

In organic chemistry, atom $^{12}_6$C can be regarded as the central atom of the hybridization principle. Therefore, as a first illustration of the new atom model the constellation of $^{12}_6$C is described (Fig. 6).

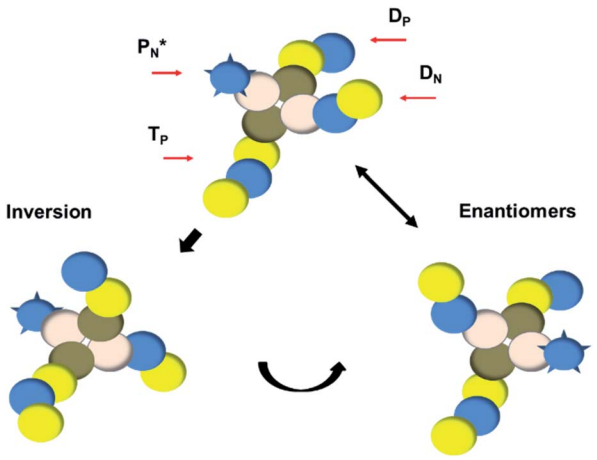

Fig. 6 Constellation of carbon atom $^{12}_6$C with $^4_2$He as building block and four different subunits: P^*_N and D_N at the anchor neutron side, D_P and T_P at the anchor proton side. Inversion and subsequent stereo isomerism of the C-atom when the C-atom bears four different chemical groups.

© 2021 The Author(s). Published by the Royal Society of Chemistry

Open Access Article. Published on 19 August 2021. Downloaded on 2/7/2026 11:39:10 PM.
This article is licensed under a Creative Commons Attribution-NonCommercial 3.0 Unported Licence.

The $^4_2$He-building block contains as subunits at the anchor neutron side a P^*_N and a D_N, at the anchor proton side a D_P and a T_P. The anchor $^4_2$He-unit can flip, leading to chemical inversion in so-called S_N2 reactions. The atom exhibits stereo isomerism in case four different chemical groups are bound to the atom: the inverted constellation is the enantiomer of the non-inverted one (Fig. 6).

2.2.1 Molecules of carbon with hydrogen and carbon. D_N and T_P are the neutron donors for the hybridization. The atom can hybridize in two ways (Fig. 6): the first mode is P^*_N with T_P and D_N with D_P. This represents the common symmetrical sp^3-hybridization and is present in the tetrahedral compound CH_4 (and covers at the same time the observed subtle difference in bond strength of the four C–H bonds of the CH_4 molecule[23]). The second mode of hybridization is P^*_N with D_N and T_P with D_P. In this hybridization mode, the distance between the anchor protons is slightly larger and is present in *e.g.* staggered carbon–carbon chains with the hybridized P^*_N/D_N bearing the hydrogen atoms.

Multiple bonds formed in the new model are intrinsically the concretization of the banana or bent bonds, whose description had already been shown to be energetically superior to the symmetry-restricted σ, π bond representation of Hückel.[24–27]

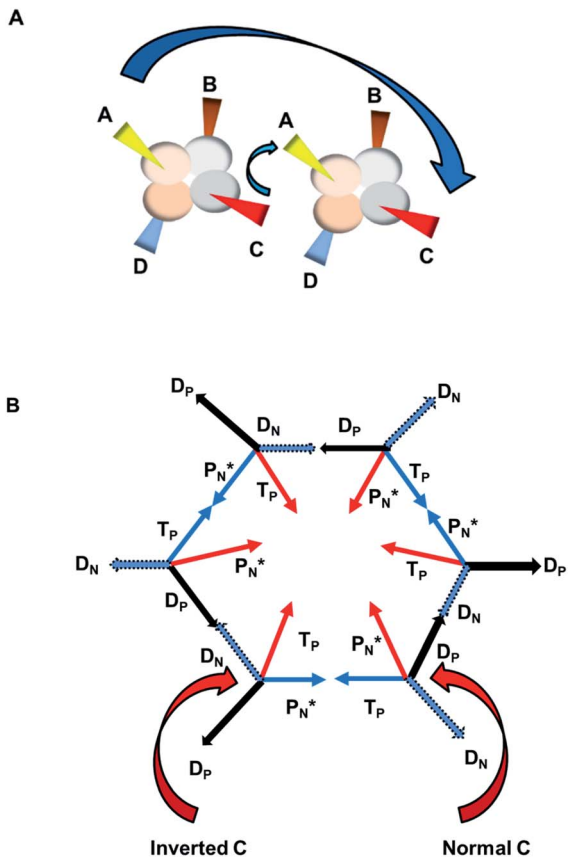

Fig. 7 (a) Principle of symmetrical double bond (AC–CA) formation between two non-inverted ("normal") carbon atoms which leaves the remaining subunits B, D in cissoid conformation; (b) combining alternatingly three "normal" with three "inverted" carbon atoms *via* a D_N–D_P bond and a symmetrical $P^*_N - T_P$ double bond creates the resonance structure of benzene.

The subunits (P_N, D_N, T_P, D_P) can form several double and triple bonds combinations, dependent on the history of the sample and the chemical group R. One may, however, expect the most energetically balanced, symmetrical molecule to be formed, especially at higher temperatures. In that case, the favorite combinations in double bonds, therefore, will be (1) D_P with T_P, and T_P with D_P, (2) P^*_N with T_P, and T_P with P^*_N or (3) D_P with D_N, and D_N with D_P. Option (1) will be the case in *e.g.* ethylene (C_2H_4) with the hydrogen atoms at the hybridized (P^*_N + D_N). Allenes provide an elegant example of option (2) and (3) in this respect, because in allenes the central carbon atom possesses both favorite symmetrical combinations, giving rise to the well-known two-bladed propeller geometry.[28]

The favorite combination in triple bonds will be D_P with T_P, T_P with D_P, and D_N with D_N wherein the neutron of T_P is hybridized with P^*_N. In *e.g.* acetylene (C_2H_2) this P^*_N bears the hydrogen atom. Molecule N_2 also possesses this triple bond combination (*vide infra*, paragraph 2.4).

The structure of benzene is an intriguing one in the new model. As shown in Fig. 7A, when a symmetrical double bond is created between A and C of two 'normal' carbon atoms, B and D end up in a *cis*-position. So formation of the symmetrical double bond P^*_N with T_P and T_P with P^*_N, leads to a *cis*-position of the D_P's (and *cis*-position for the D_N's). The same symmetrical double bond, but with one of the carbon atoms inverted, leads to a *trans*-position of the D_P's. By combining alternatingly three "normal" and three "inverted" carbon atoms in the way shown in Fig. 7B, for benzene a fascinating structure is obtained wherein a double bond between P^*_N and T_P can be formed to the left and to the right. Or in other words, a resonance system is created that answers the famous Kekulé benzene-structure problem from 1865.[29,30] Other examples of $P^*_N - T_P$ resonance, namely between C and O, will be dealt with in paragraph 2.4.

2.2.2 Carbon isotopes. Compared with $^{12}_6$C, atom $^{13}_6$C bears a D^*_N instead of a P^*_N. This constellation of a carbon atom appears to be stable also, but the abundancy of $^{13}_6$C is not high (1.1% abundance) (Fig. 8).

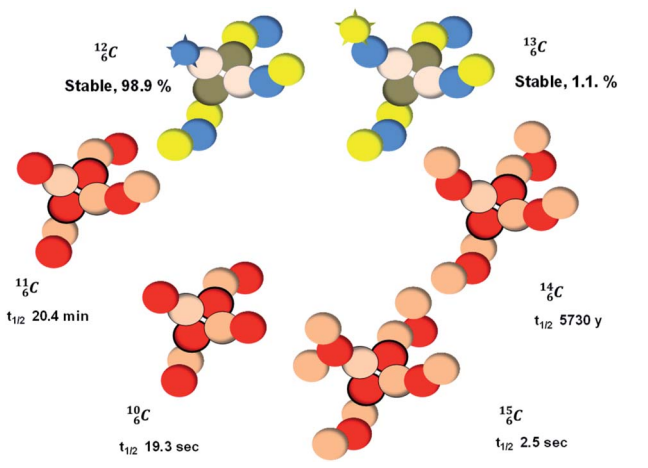

Fig. 8 Constellation of the main isotopes of carbon ($1s^2\ 2s^2\ 2p^2$) in the new model.

Open Access Article. Published on 19 August 2021. Downloaded on 2/7/2026 11:39:10 PM.
This article is licensed under a Creative Commons Attribution-NonCommercial 3.0 Unported Licence.

The well-known long-living carbon isotope $^{14}_{6}$C ($t_{1/2}$ of 5730 y, decays to $^{14}_{7}$N) bears two D_N's and two T_P's. In the $^{15}_{6}$C atom there is no obvious place for the additional neutron: an exotic T_N is formed, and this isotope decays immediately ($t_{1/2}$ 2.5 s, decays to $^{15}_{7}$N). Radioisotope $^{11}_{6}$C ($t_{1/2}$ 20.4 min, decays to $^{11}_{5}$B) bears, compared to $^{12}_{6}$C, a D_P instead of a T_P, while in radioisotope $^{10}_{6}$C ($t_{1/2}$ 19.3 s, decays to $^{10}_{5}$B) also the neutron at the D_N is missing (Fig. 8). From the latter constellation, it can be concluded that $^{10}_{6}$C is the last carbon isotope that can chemically react as carbon. For the radioisotopes $^{9}_{6}$C and $^{8}_{6}$C there is no obvious place for the proton, and these radioisotopes are therefore extremely fast deteriorating nuclei, ending up as α-particles, mostly *via* proton loss.

In the new atom model, the weak nuclear force is transformed into a stability rule for each anchor side. The carbon isotopes $^{12}_{6}$C and $^{13}_{6}$C allow the deriving of these stability rules. The summarized subunits at the anchor proton side of the carbon isotopes $^{12}_{6}$C and $^{13}_{6}$C give $n = 3, p = 2$, with n for neutron and p for proton. When $n = 2, p = 2$ ($^{10}_{6}$C, $^{11}_{6}$C) or $n = 4, p = 2$ ($^{14}_{6}$C, $^{15}_{6}$C), the atom is instable. So our new model indicates that in order to be stable, the summarized number of neutrons at the anchor proton side should exceed that of protons by exactly one *i.e.* should follow the stability rule $n = p + 1$. Applying the same approach for the anchor neutron side, and counting a square neutron or proton for $\frac{1}{2}$, the stability rule for $^{12}_{6}$C and $^{13}_{6}$C appears to be $n = \mathrm{p} - \frac{1}{2}$, namely $n = 1, p = 1\frac{1}{2}$ for $^{12}_{6}$C and $n = 1\frac{1}{2}, p = 2$ for $^{13}_{6}$C. Because radioisotopes produced in a cyclotron or neutron generator do not contain square protons or square neutrons (*vide supra* 1.1), the four carbon radioisotopes $^{10}_{6}$C, $^{11}_{6}$C, $^{14}_{6}$C and $^{15}_{6}$C deviate from the anchor neutron stability rule as well. In the new atom model, conversion will, therefore, take place until the new-born constellations comply to both rules.

2.3 The elements $Z = 1$–6

For an insight in how we arrived at the $^{12}_{6}$C atom constellation, and for a demonstration of the general applicability of the stability rules, first a short overview of the atom configuration of the elements with $Z = 1$–6 in the new model.

2.3.1 The 1s and 1s²-elements H and He ($Z = 1$ and $Z = 2$).

The simplest of nuclei to demonstrate the transfer of a newborn proton after conversion of a neutron into a proton is the β⁻-emitting radioisotope $^{3}_{1}$H ($t_{1/2}$ 12.3 y), also called tritium, and its daughter $^{3}_{2}$He (Fig. 9).

At the same time, the $^{3}_{2}$He-atom can be taken as the prototype of an atom that bears a square proton (Fig. 9). Because of this square proton, the $^{3}_{2}$He-atom is stable and in fact it is the only stable atom in the periodic system with more protons than neutrons. Its abundancy is only 1.34×10^{-4}%, so most probably originating solely from the decay of cosmic-produced $^{3}_{1}$H. With the noble gas $^{4}_{2}$He, a unit consisting of two neutrons and two protons alternatingly linked with each other, the first row ends. When adding an additional neutron at the anchor proton side, forming $^{5}_{2}$He, the neutron is immediately emitted ($t_{1/2}$ 0.7 × 10^{-21} s).

2.3.2 The 1s²2s- and 1s²2s²-elements Li and Be ($Z = 3$ and $Z = 4$).

With $^{4}_{2}$He as building block, it appears that the addition of a proton as the only subunit is not accepted (Fig. 9): from the thus assembled $^{5}_{3}$Li the proton is immediately emitted ($t_{1/2}$ 0.4 × 10^{-21} s). Adding a proton to the anchor neutron side requires compensation in the form of a neutron at the anchor proton side. What is more, the latter new neutron as well as the new proton are shared to evenly divide the burden of the new situation. With this shared neutron between the anchor protons, two stable isotopes of lithium exist: $^{6}_{3}$Li (abundancy 7.6%) bearing a shared P^{*}_{N} at the anchor neutron side, and $^{7}_{3}$Li (abundancy 92.4%) bearing a shared D^{*}_{N} at the anchor neutron side (Fig. 10 and 11).

Introduction of a neutron at each anchor proton is too much: when the anchor proton side of $^{6}_{3}$Li is hit by a neutron the composite atom breaks down into $^{3}_{1}$H and an α-particle (a $^{4}_{2}$He-unit),[31] whereas with the (n, γ) reaction on $^{7}_{3}$Li, giving $^{8}_{3}$Li, a radioisotope with a $t_{1/2}$ of 0.8 s is produced.[32]

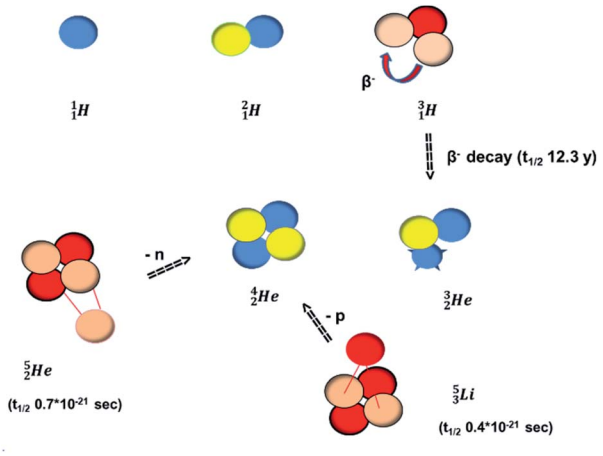

Fig. 9 Constellation of the main isotopes of hydrogen (1s), helium (1s²) and $^{5}_{3}$Li in the new model, including transfer of the newborn proton during decay in case of $^{3}_{1}$H (red lines represent artificial distance, drawn for the sake of clarity; curved arrow indicates conversion plus shift).

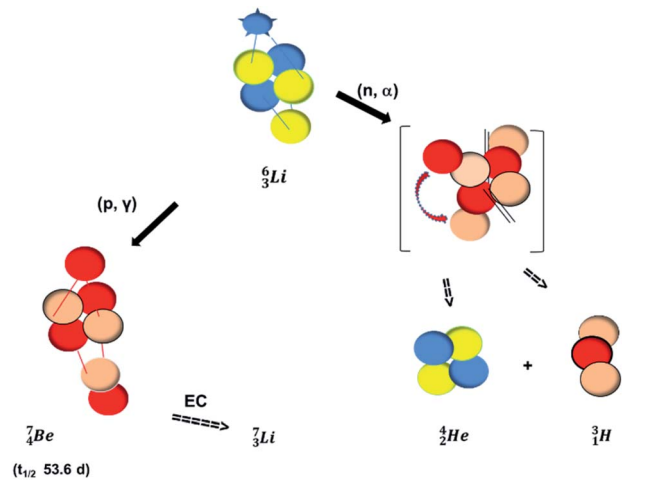

Fig. 10 Constellation of $^{6}_{3}$Li (1s²2s) in the new model, including the decomposition of $^{6}_{3}$Li upon bombardment by neutrons and an illustrative production route to $^{7}_{4}$Be (red and blue lines represent artificial distance drawn for the sake of clarity, curved red puckered arrow indicates recombination, double black lines represent breakage).

© 2021 The Author(s). Published by the Royal Society of Chemistry

Open Access Article. Published on 19 August 2021. Downloaded on 2/7/2026 11:39:10 PM.
This article is licensed under a Creative Commons Attribution-NonCommercial 3.0 Unported Licence.

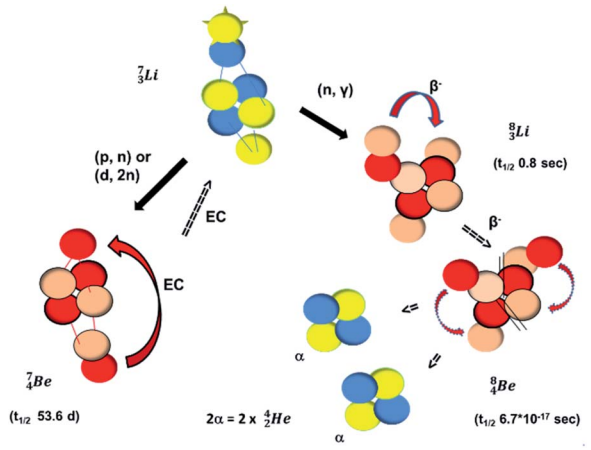

Fig. 11 Constellation of $^{7}_{3}$Li ($1s^2 2s$) in the new model, including the decomposition of $^{7}_{3}$Li upon bombardment by neutrons and two additional illustrative production routes to $^{7}_{4}$Be (red and blue lines represent artificial distance, curved red arrows indicate conversion plus shift, curved red puckered arrows indicate recombination, double black lines represent breakage).

Concerning the stability rules, $^{6}_{3}$Li and $^{7}_{3}$Li both follow the new rules, with $n = 1, p = 0$ at the anchor proton side, and $n = 0$, $p = \frac{1}{2}$ and $n = \frac{1}{2}$, $p = 1$ at the anchor neutron side, respectively. $^{8}_{3}$Li possesses with $n = 2$, $p = 0$ at the anchor proton side a neutron too much. Notably, for $^{5}_{2}$He and $^{5}_{3}$Li neither β^--decay nor β^+-decay leads to a stable situation, leaving emission of the additional neutron and proton, respectively, as the only option.

The beryllium (Be) isotopes reveal that the requirements for the addition of the second proton onto the $^{4}_{2}$He backbone are also very stringent and delicate (Fig. 12). At the anchor proton side, only a constellation wherein the shared neutron is replaced by a shared T_P appears acceptable, whereas at the anchor neutron side only a shared D^*_N is accepted, yielding the $^{9}_{4}$Be atom (100% abundancy).

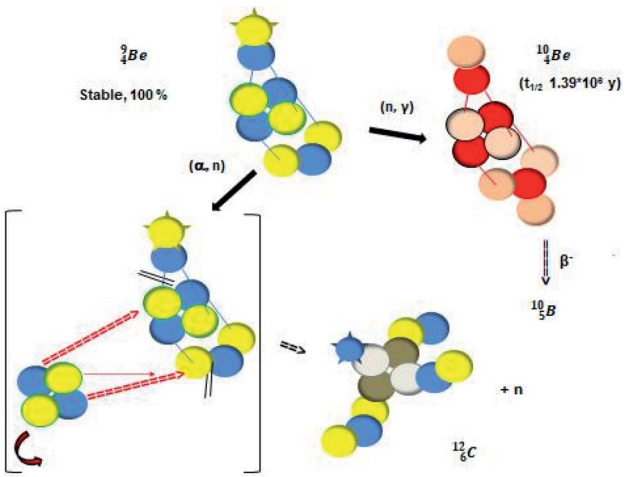

Fig. 12 Constellation of $^{9}_{4}$Be ($1s^2 2s^2$) in the new model, including formation of $^{10}_{4}$Be upon bombardment by neutrons and formation of $^{12}_{6}$C upon bombardment by alpha's (discovery of the neutron) (red arrows indicate point of attack, red and blue lines represent artificial distance, double black lines represent breakage).

The proposed $^{9}_{4}$Be-configuration deviates from the Aufbau principle, but is perfectly in accordance with the chemistry of Be: linear molecular geometry *i.e.* formation of linear compounds. In addition, $^{9}_{4}$Be follows with its $n = 2$, $p = 1$ at the anchor proton side, and its $n = \frac{1}{2}$, $p = 1$ at the anchor neutron side the stability rules.

Whereas for lithium the constellation with a shared P^*_N at the anchor neutron side ($^{6}_{3}$Li) is already a minority, such constellation for beryllium, *i.e.* $^{8}_{4}$Be, does not exist. Radioisotope $^{8}_{3}$Li ($t_{1/2}$ of 0.8 s)[33] converts its D_N-neutron into a proton at one of the N_P's, producing an extremely unstable ($t_{1/2}$ 6.7×10^{-17} s) sort of "open" $^{8}_{4}$Be, an atom that, instead of recombining into a constellation with a shared P^*_N and shared T_P, energetically prefers to break down into two α-particles (Fig. 11). A similar sort of break down was observed for the composite atom produced by neutron bombardment of $^{6}_{3}$Li (Fig. 10). Radioisotope $^{8}_{3}$Li is not the only radioisotope that ends up as α-particles in this way: the boron radioisotopes $^{8}_{5}$B, after β^+-decay, and $^{9}_{5}$B, after proton emission, also end up as α-particles *via* this "open" $^{8}_{4}$Be (*vide infra*). Radioisotope $^{7}_{4}$Be is an unstable Be-isotope with a shared D_P between the anchor protons. It can be produced *via* a (p, γ) reaction on $^{6}_{3}$Li[34] and *via* a (p, n)[35] or (d, 2n)[36] reaction on $^{7}_{3}$Li (Fig. 10 and 11). The impact of the proton takes place at the shared neutron between the anchor protons. In the case of the (p, n) on $^{7}_{3}$Li, the neutron at the D^*_N is thrown out; in the (d, 2n) reaction, the second neutron is the neutron from the deuterium particle that is turned aside without interaction with the nucleus. With a $t_{1/2}$ of 53.6 d, the proton of the shared D_P at the anchor proton side of $^{7}_{4}$Be is converted into a square neutron at the shared P_N, giving $^{7}_{3}$Li.

In radioisotope $^{10}_{4}$Be, produced by a (n, γ) reaction on $^{9}_{4}$Be,[37] the shared T_P -proton bears a neutron. The atom is unstable, decaying to $^{10}_{5}$B (*vide infra*), but it is a very slow conversion ($t_{1/2}$ 1.39×10^6 y), most likely owing to the balance and symmetry in the constellation. For radioisotope $^{11}_{4}$Be, there is no obvious place for the additional neutron: an exotic T_N is formed, yielding a very unstable isotope ($t_{1/2}$ 13.7 s), decaying to $^{11}_{5}$B (*vide infra*).

The discovery of the neutron in 1932 by Chadwick came from α-bombardment of $^{9}_{4}$Be, producing $^{12}_{6}$C.[38] As illustration of our model, nuclear bombardment with α's or nuclear transformations in which an α-particle is eliminated from the atom, provide in general too many possibilities to be used as proof by logical argument. But because the α-impact on the $^{9}_{4}$Be atom from four sides is the same, in this special case we refer to Chadwick's groundbreaking experiment. Upon α-bombardment of $^{9}_{4}$Be, the impact of the two α-protons takes place at the anchor neutron and at the neutron at the anchor proton side (Fig. 12). The shared D_N and T_P subunits at the anchor neutron and anchor proton side break open at the side of the impact. One deuteron-fragment from the α-particle binds at the freed N_P-neutron at the anchor proton side, the proton of the second deuteron part from the α-particle is incorporated at the freed anchor neutron while the remaining neutron of the second

Open Access Article. Published on 19 August 2021. Downloaded on 2/7/2026 11:39:10 PM.
This article is licensed under a Creative Commons Attribution-NonCommercial 3.0 Unported Licence.

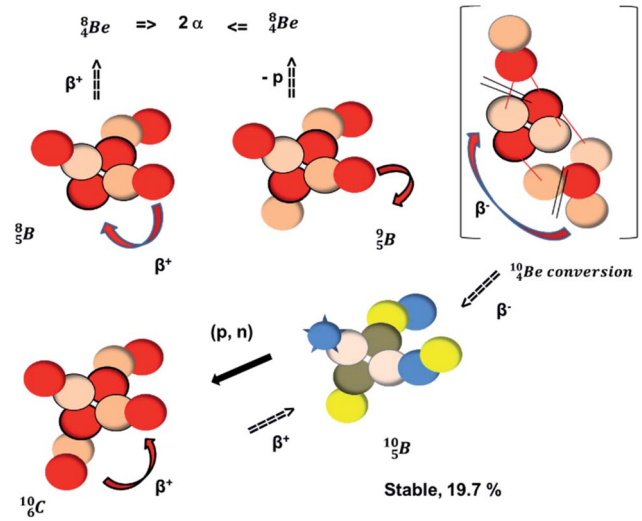

Fig. 13 Constellation of stable $^{10}_{5}B$ ($1s^2 2s^2 2p$) and of radioactive $^{8}_{5}B$ and $^{9}_{5}B$ in the new model, including conversions and some illustrative production routes.

deuteron part of the α-particle is turned aside without interaction with the nucleus.

2.3.3 The $2s^2 2p$- and $2s^2 2p^2$-elements B and C ($Z = 5$ and $Z = 6$). The element boron is the second element whose constellation deviates from the Aufbau principle. Over and above that, the isotopes $^{10}_{5}B$ and $^{11}_{5}B$ are the first stable atoms that contain four separated subunits: both atoms bear a D_N, an N_P and a D_P, whereas $^{10}_{5}B$ bears as the fourth a P^*_N, $^{11}_{5}B$ a D^*_N (Fig. 13 and 14). Consequently, the chemical versatility is increased. At the anchor proton side, the D_P can combine with the N_P and form a (formal) plus situation analogous to the one at the anchor proton side of $^{9}_{4}Be$. In combination with the D_N and the $P^*_N(^{10}_{5}B)$ or $D^*_N(^{11}_{5}B)$ at the anchor neutron side, this leads to the typical trigonal planar molecular geometry of boron compounds. Furthermore, the sole N_P represents the empty orbital of boron that exhibits chemical reactivity. N_P is capable of binding neutron-deficient ligands like water (as $BF_3 \cdot H_2O$) or F^- (as BF_4^-) with tetrahedral-like molecular geometry (see also paragraph 2.5).

Upon bombardment of $^{10}_{5}B$ with protons, a (p, n) reaction gives the short living $^{10}_{6}C$ ($t_{1/2}$ 19.5 s).[39] This $^{10}_{6}C$ converts back to $^{10}_{5}B$ *via* β^+-decay, which means that the $^{10}_{5}B$ atom is formed as daughter isotope from $^{10}_{4}Be$ as well as from $^{10}_{6}C$. In case of $^{10}_{4}Be$, the neutron of the shared T_P at the anchor proton side converts into a square proton at the anchor neutron side, while during this process the shared T_P and shared D_N break open (Fig. 13). In case of $^{10}_{6}C$, one of the D_P protons converts into a neutron (β^+-decay) and forms a D_N with one of the P_N's.

Upon bombardment of $^{11}_{5}B$ with protons, a (p, n) reaction gives radioisotope $^{11}_{6}C$ (Fig. 14).[40] This carbon radioisotope converts back to $^{11}_{5}B$ *via* β^+-decay. Radioisotopes $^{8}_{5}B$, $^{9}_{5}B$ and $^{12}_{5}B$ are very instable isotopes: $^{8}_{5}B$ (β^+-decay) and $^{9}_{5}B$ (proton emission) end up *via* $^{8}_{4}Be$ as α-particles, while $^{12}_{5}B$ decays to $^{12}_{6}C$ with a $t_{1/2}$ of 0.02 s. The short half-life of radioisotope $^{12}_{5}B$, that is produced by a (d, p) reaction on $^{11}_{5}B$,[41] confirms that two full D_N's at the anchor neutron side together with the fact that the anchor proton side bears three neutrons *versus* one proton, give rise to severe instability.

Both stable boron isotopes $^{10}_{5}B$ and $^{11}_{5}B$ fit with the stability rules, with their $n = 2, p = 1$ at the anchor proton side, and its $n = 1$, $p = 1\frac{1}{2}$ and its $n = 1\frac{1}{2}$, $p = 2$ at the anchor neutron side, respectively.

2.4 Nitrogen ($Z = 7$), oxygen ($Z = 8$) and their lone pairs

2.4.1 Nitrogen. With the atoms nitrogen (N) and oxygen (O) we now arrive at the lone pair principle of the new model. It appears that the $^{14}_{7}N$ atom at the anchor neutron side possesses as lone pair a $^{3}_{2}He$-unit with a square proton (Fig. 15). Nitrogen is the first atom, since Li, that follows the Aufbau principle again ($1s^2 2s^2 2p^3$). Fig. 15 also shows the constellation of the stable $^{15}_{7}N$ (0.4% abundance), of the instable $^{16}_{7}N$ ($t_{1/2}$ 7.1 s, decays to $^{16}_{8}O$) and of the instable $^{13}_{7}N$ ($t_{1/2}$ 9.96 min, decays to $^{13}_{6}C$). The $^{16}_{7}N$ isotope is produced by a (n, γ) or (d, p) on $^{15}_{7}N$,[42,43] and by a (n, p) on $^{16}_{8}O$.[44] These impacts give insight in the

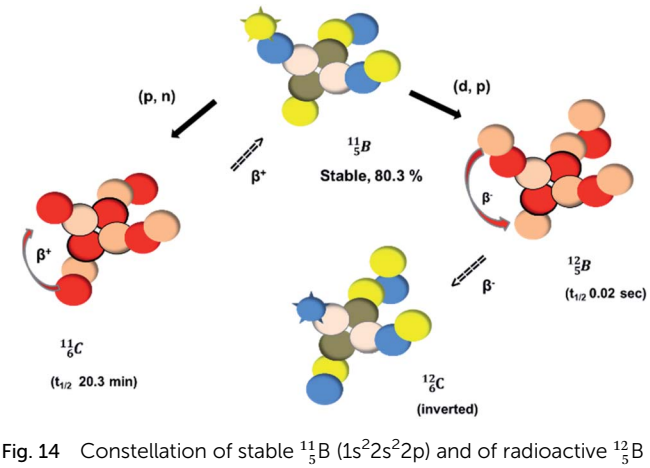

Fig. 14 Constellation of stable $^{11}_{5}B$ ($1s^2 2s^2 2p$) and of radioactive $^{12}_{5}B$ in the new model, including conversions and two illustrative production routes.

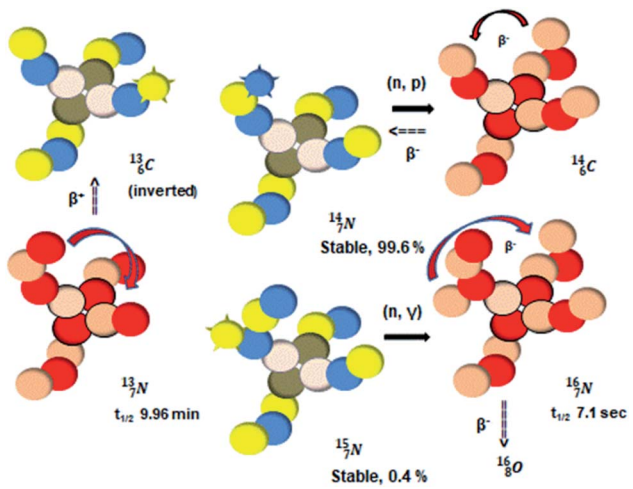

Fig. 15 Constellation of the main isotopes of nitrogen ($1s^2 2s^2 2p^3$) in the new model, including conversions.

© 2021 The Author(s). Published by the Royal Society of Chemistry

Open Access Article. Published on 19 August 2021. Downloaded on 2/7/2026 11:39:10 PM.
This article is licensed under a Creative Commons Attribution-NonCommercial 3.0 Unported Licence.

position of the second lone pair in the constellation of oxygen (see Fig. 18 in the next paragraph). Atoms $^{14}_{7}$N and $^{15}_{7}$N both have $n = 3$, $p = 2$ at the anchor proton side, just like $^{12}_{6}$C and $^{13}_{6}$C. At the anchor neutron side it is $n = 2$, $p = 2\frac{1}{2}$ for $^{14}_{7}$N, for $^{15}_{7}$N it is $n = 2\frac{1}{2}$, $p = 3$. So both constellations obey the derived stability rules.

Radioactive $^{13}_{7}$N is produced in a cyclotron in various ways (Fig. 16). It is therefore an effectual isotope to demonstrate the consistency of the adjusted atom model in the field of isotope production.

The $^{13}_{7}$N atom is produced *via* a (α, n) on $^{10}_{5}$B,[45–47] a (d, n) or (p, γ) on $^{12}_{6}$C,[41b,48–50] a (p, n) on $^{13}_{6}$C,[51] a (p, d) on $^{14}_{7}$N[52] and a (p, α) on $^{16}_{8}$O[51] (Fig. 16). In all cases, the impact takes place at the D_N-unit (for $^{10}_{5}$B the impact takes place at the D_N-unit and the N_P-unit in the way described for the α-bombardment of $^{9}_{4}$Be, producing $^{12}_{6}$C). The D_N is converted into a $^{3}_{2}He_N$-unit containing a full energy proton (not a square one), which leads to a fast decay ($n = 1$, $p = 3$ at the anchor neutron side). After proton impact on $^{13}_{6}$C, $^{14}_{7}$N and $^{16}_{8}$O, the rule "last in, first out" is followed: for $^{13}_{6}$C the square neutron of the D^*_N is thrown out, for $^{14}_{7}$N the D^*-fragment from the $^{3}_{2}He^*_N$-unit, while for $^{16}_{8}$O the thrown-out α-particle consists of the deuteron-parts from the $^{4}_{2}He_P$- and $^{3}_{2}He^*_N$-unit (see next paragraph for the configuration of $^{16}_{8}$O). In the case of $^{12}_{6}$C as target material, the combined (d, n) and (p, γ) bombardment,[48,49] both producing the same $^{13}_{7}$N, indicate that the proton of the incoming deuteron is built in and its neutron is turned aside without interaction with the nucleus. Notably, for $^{10}_{5}$B and $^{12}_{6}$C an additional consequence of the impact at D_N is the activation of P^*_N into a full energy proton.

The $^{14}_{6}$C atom, either produced in a neutron generator or in the cosmos, comes from a (n, p) reaction on $^{14}_{7}$N (Fig. 15).[53] The neutron is incorporated onto the D_P of the $^{14}_{7}$N-atom, while throwing out the square proton of the $^{3}_{2}He^*_N$-unit, whereas $^{14}_{6}$C decays back to $^{14}_{7}$N by converting the neutron of the newborn T_P into a square proton at the D_N, forming the $^{3}_{2}He^*_N$-unit.

Lastly, atom $^{11}_{6}$C is, in addition to a (p, n) reaction on $^{11}_{5}$B, also produced *via* a (p, α) reaction on $^{14}_{7}$N.[54] This (p, α) on $^{14}_{7}$N giving $^{11}_{6}$C, implies the impact of the proton at the T_P of the $^{14}_{7}$N atom. The thrown-out α-particle consists of the deuteron parts from the $^{3}_{2}He_N$- and the T_P-unit. Thereby these two carbon isotope productions also follow the rule "last in, first out".

2.4.2 Molecules of nitrogen with hydrogen and carbon. In NH_3 (gas), the $^{3}_{2}He^*_N$-unit is a chemically quietened lone pair by hybridization with T_P, while D_N and D_P are hybridized as in the CH_4-molecule. These hybridized couples can easily flip, leading to the well-known pyramidal inversion of NH_3. In the new model no spontaneous tunneling of hydrogen atoms is required.[55,56] Notably, in N_2, the $^{3}_{2}He^*_N$-unit is also chemically quietened *via* hybridization with T_P, and the triple bond of the N_2-molecule consists of two mutual D_P–T_P bonds plus a D_N–D_N bond. In NH_4^+, T_P is hybridized with D_P. At the anchor neutron side, the square proton of the $^{3}_{2}He^*_N$-unit is hybridized with the neutron of D_N, forming a symmetrical bridgehead at the anchor neutron side.

The full-energy proton of the $^{3}_{2}He^*_N$-unit forms the fourth NH-bond (Fig. 17A), whereas the square proton has turned over its electron to this latter hydrogen atom. Notably, the oxygen atom (see next paragraph) can even force both protons of the $^{3}_{2}He^*_N$-unit into covalent bond formation, demonstrating the versatility of the $^{3}_{2}He^*_N$-unit.

In combination with carbon, the intriguing existence of *Z* and *E* (formerly called *syn* and *anti*) isomers for N-alkyl substituted imines ($R^1R^2C{=}NR^3$) provides a telling example.[57–59] The stereo-isomerism originates from the fact that the double bond between carbon and nitrogen is a symmetrical one (carbon–D_P with nitrogen–D_N, carbon–D_N with nitrogen–D_P), but with either a "normal" or an "inverted" nitrogen atom (Fig. 6 and 7A).

2.4.3 Oxygen. In Fig. 18, the constellation is depicted of the stable oxygen isotopes $^{16}_{8}$O (abundance 99.76%), $^{17}_{8}$O (abundance

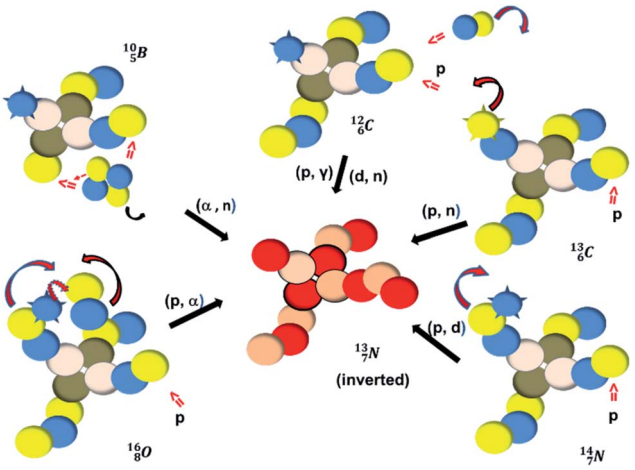

Fig. 16 Illustration of the consistency in production routes in the new model illustrated by production of $^{13}_{7}$N (red arrows indicate the point of impact).

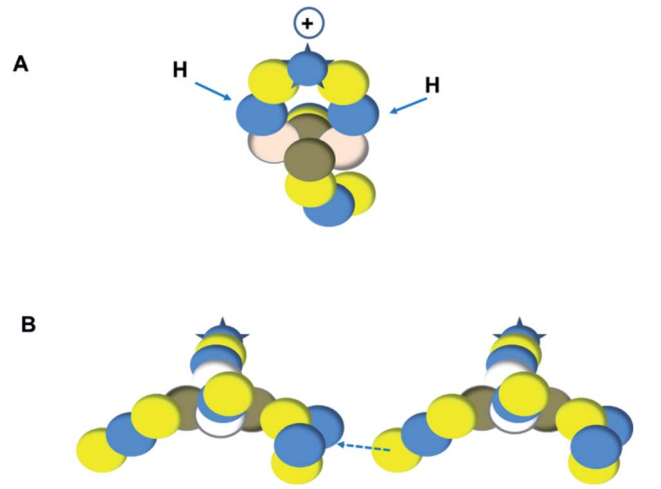

Fig. 17 Special lone pairs of nitrogen and oxygen: (A) formation of a bridgehead between the $^{3}_{2}He^*_N$-lone pair and the D_N of the nitrogen or oxygen atom, giving rise to the distorted tetrahedral NH_4^+ or H_3O^+ molecule (hydrogens at the anchor proton side are not shown); (B) the formation of a "hydrogen bond" *via* a neutron link between the oxygen–T_P of a H_2O molecule and the neutron-deficient $^{4}_{2}He_P$-lone pair of the oxygen atom of a neighboring H_2O molecule (dashed blue arrow means formation of hydrogen bond).

Open Access Article. Published on 19 August 2021. Downloaded on 2/7/2026 11:39:10 PM.
This article is licensed under a Creative Commons Attribution-NonCommercial 3.0 Unported Licence.

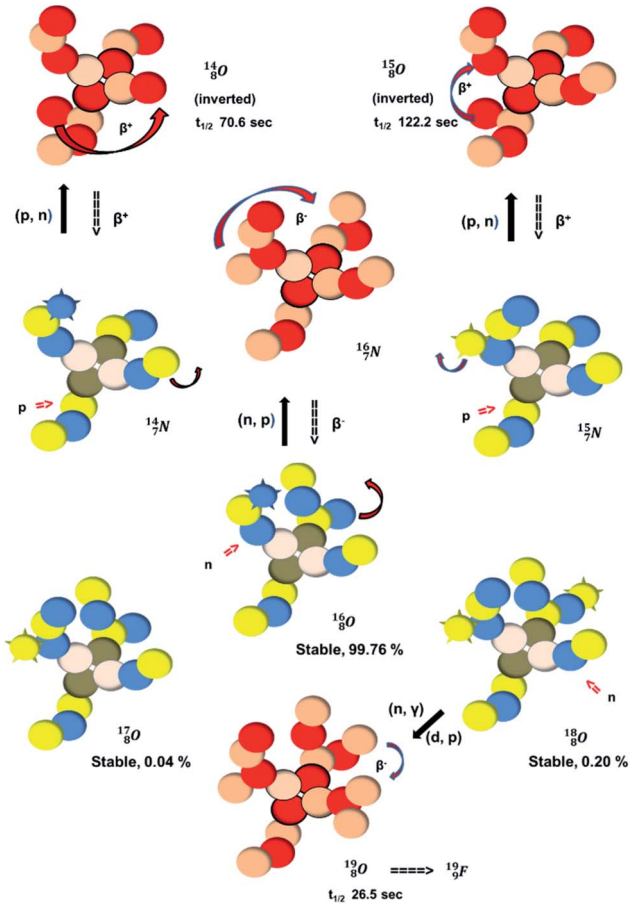

Fig. 18 Constellation of the main isotopes of oxygen ($1s^2$ $2s^2$ $2p^4$) in the new model, including production and conversion of the instable ones.

0.04%) and $^{18}_{8}O$ (abundance 0.2%), together with that of the instable oxygen isotopes $^{14}_{8}O$ ($t_{1/2}$ 70.6 s), $^{15}_{8}O$ ($t_{1/2}$ 122.2 s) and $^{19}_{8}O$ ($t_{1/2}$ 26.5 s).

The main oxygen isotope $^{16}_{8}O$ bears at the anchor neutron side the same D_N and the same versatile $^{3}_{2}He^{*}_{N}$-unit as described above for $^{14}_{7}N$, so $n = 2$, $p = 2\frac{1}{2}$. It differs, however, from $^{14}_{7}N$ by bearing a $^{4}_{2}He_P$-unit at the anchor proton side instead of a D_P. This $^{4}_{2}He_P$ lone pair possesses an intriguing property, it is slightly neutron-deficient and is not closed yet ("open" lone pair). The $^{4}_{2}He_P$-unit is chemically closed upon interaction with an additional neutron, but not necessarily a neutron from its own constellation. The water molecule forms a beautiful illustration of this latter aspect (*vide infra*). Notably, one of the protons of this $^{4}_{2}He_P$-unit is thrown out in the (n, p) reaction on $^{16}_{8}O$, producing $^{16}_{7}N$ (see Fig. 18).

With regard to other nuclear aspects, $^{16}_{8}O$ and $^{17}_{8}O$ bear with $n = 4$, $p = 3$ at the anchor proton side exactly one neutron more than the number of protons, obeying the stability rule. Atom $^{17}_{8}O$ possesses the same anchor neutron subunits as $^{15}_{7}N$. Atom $^{18}_{8}O$ is as neutron-saturated as $^{14}_{6}C$ and $^{10}_{4}Be$ are. The latter radioisotopes slowly convert a neutron into a proton, yielding $^{14}_{7}N$ and $^{10}_{5}B$, respectively. In case of the $^{18}_{8}O$ isotope, however, conversion of a neutron into a proton yielding $^{18}_{9}F$, does not occur. In fact, it is the other way around: radioactive $^{18}_{9}F$ decays to $^{18}_{8}O$ In $^{18}_{8}O$ its tenth neutron appears to remain as a square neutron in the $^{4}_{2}He_P$-lone pair, as $^{5}_{2}He^{*}_{P}$-unit. With that, $^{18}_{8}O$ is the first example of an isotope that is stable, despite its $n = 4\frac{1}{2}$, $p = 3$ at the anchor proton side *i.e.* the first isotope that follows a special anchor proton side stability rule, namely $n = p + 1\frac{1}{2}$.

For the $^{19}_{8}O$ atom, produced either by a (n, γ) or (d, p) reaction on $^{18}_{8}O$,[60,61] or a (n, p) on $^{19}_{9}F$,[62] there is, like $^{15}_{6}C$, no obvious place for the additional neutron, so again an exotic T_N is formed. This $^{19}_{8}O$ isotope quickly decays ($t_{1/2}$ 26.5 s) to $^{19}_{9}F$ *via* conversion of the neutron of the $^{5}_{2}He_P$-unit into a proton onto this T_N. Isotope $^{15}_{8}O$ is produced *via* a (p, n) reaction on enriched $^{15}_{7}N$.[63] The proton impact takes place at the T_P while the square neutron of the $^{4}_{2}He^{*}_{N}$-unit is thrown out (so again last in, first out). Its short half live ($t_{1/2}$ 122.2 s, converts back to $^{15}_{7}N$ *via* β^+-decay) demonstrates that a $n = 3$, $p = 3$ at the anchor proton side is an unacceptable situation. Atom $^{14}_{8}O$ ($t_{1/2}$ 70.6 s) is the last atom configuration that may chemically act like oxygen and decays to $^{14}_{7}N$ Atoms $^{13}_{8}O$ and $^{12}_{8}O$ are extremely unstable, these decay to $^{13}_{6}C$ or $^{12}_{6}C$, and $^{11}_{5}B$ or $^{10}_{5}B$, respectively, *via* β^+ and/or proton emission.

2.4.4 Molecules of oxygen with hydrogen (O with H). In H_2O, the T_P and D_N of the oxygen atom bear the hydrogen atom. In alkaline solutions, the OH^--group has lost its hydrogen atom at the T_P. In acidic solutions, producing the H_3O^+-molecule, the square proton of the oxygen $-\ ^{3}_{2}He^{*}_{N}$-unit is hybridized with the neutron of the oxygen-D_N, forming a symmetrical bridgehead at the anchor neutron side as in NH_4^+. The full-energy proton of the oxygen $-\ ^{3}_{2}He^{*}_{N}$-unit has formed the third OH-bond (Fig. 17A).

As a gas, the oxygen atom in H_2O is hybridized *via* T_P with the $^{3}_{2}He^{*}_{N}$-unit and D_N with the $^{4}_{2}He_P$-unit. As such, the H_2O molecule perfectly fits with the four different energy levels (2 OH-peaks, 2 lone pair peaks) observed in the photo-electronic spectra of H_2O ("no rabbit ears on the water").[64]

As a liquid, H_2O is a temperature-dependent mixture of the gas-phase hybridized form and a hybridized form in which the $^{3}_{2}He^{*}_{N}$-unit is linked with D_N, and in which the T_P is not linked intra-atomic with the $^{4}_{2}He_P$-unit, but with the $^{4}_{2}He_P$-unit of a neighboring water molecule (Fig. 17B). Such an energetically favorable closure of the $^{4}He_p$-unit by a neighboring neutron is the basis for hydrogen bonds, hydrates, and *e.g.* crystal water.

As a solid (around zero degrees and lower), the predominant form of H_2O will be the fully de-hybridized one, *i.e.* neutron ("hydrogen") bonds between T_P and the $^{4}_{2}He_P$-unit or $^{3}_{2}He^{*}_{N}$-unit of a neighboring water molecule, and neutron bonds between D_N and the $^{3}_{2}He^{*}_{N}$-unit or $^{4}_{2}He_P$-unit of a neighboring water molecule. This fully de-hybridized form of the water molecule corresponds with expansion, which means a change in volume and, therefore, a change in density. Dissolved cations, but also the $^{17}_{8}O$ isotope with a square neutron at the $^{3}_{2}He_N$-unit and the $^{18}_{8}O$ isotope with an additional square neutron at the $^{4}_{2}He_P$-unit (see Fig. 18) will of course disrupt this hydrogen bond network, and might well be part of the reason behind the geometric variation in hexagonal-shaped snowflakes.

© 2021 The Author(s). Published by the Royal Society of Chemistry

Open Access Article. Published on 19 August 2021. Downloaded on 2/7/2026 11:39:10 PM.
This article is licensed under a Creative Commons Attribution-NonCommercial 3.0 Unported Licence.

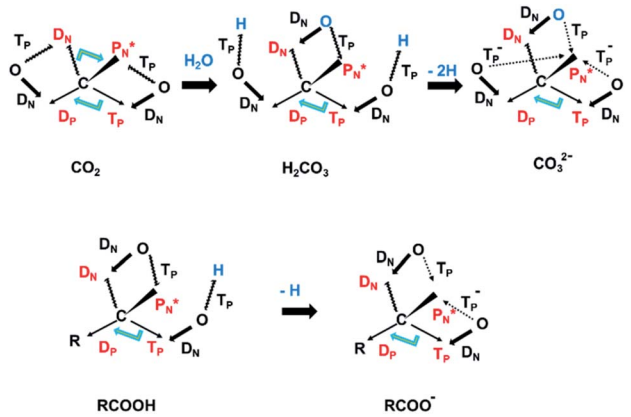

Fig. 19 Some illustrative carbon–oxygen combinations in the new model: (a) CO_2; (b) H_2CO_3 and resonance in CO_3^{2-}; (c) RCOOH and resonance in $RCOO^-$ (blue hooked arrow indicates hybridization).

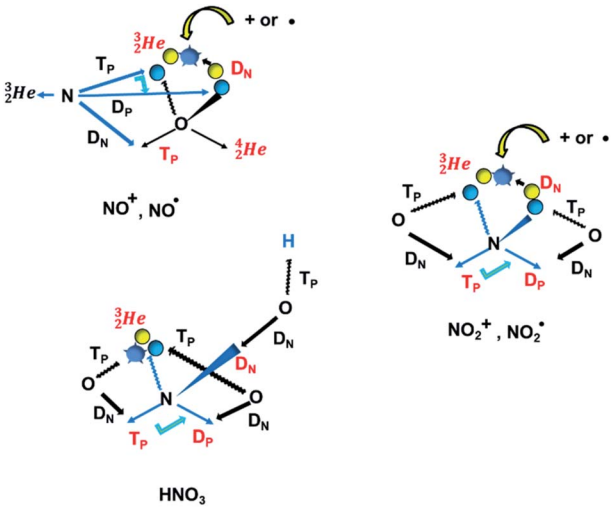

Fig. 20 Some illustrative nitrogen-oxygen combinations in the new model: (a) $NO^+/NO^•$; (b) $NO_2^+/NO_2^•$; (c) HNO_3.

2.4.5 Molecules of oxygen with carbon (O with C). From the various combinations of oxygen with carbon, Fig. 19 gives a few typical examples.

In carbon dioxide (CO_2), the D_N of each oxygen atom is bound to the hybridized carbon ($T_P + D_P$), the T_P of each oxygen atom is bound to the hybridized carbon ($P_N^* + D_N$). Upon dissolving of CO_2 in water, carbonic acid (H_2CO_3) is formed. In this process, the two oxygen T_P's become detached from the carbon ($P_N^* + D_N$), forming two OH-groups, while the oxygen of the incoming H_2O molecule becomes bound with its T_P to the carbon P_N^* and with its D_N to the carbon D_N.

In ketones, aldehydes and carboxylic acids the double-bonded oxygen atom is bound in the same way to carbon's P_N^* and D_N, whereas the anchor proton side of that C-atom is hybridized into the ($T_P + D_P$) form. Keto–enol tautomerism and chemical attack on ketones take place at P_N^* whereby the oxygen-T_P of the double-bonded oxygen becomes OH or O^-. In carboxylic acids (RCOOH), the OH-group is bound with its oxygen–D_N to the hybridized carbon ($T_P + D_P$). The oxygen–T_P of this OH-group loses its hydrogen relatively easily because the oxygen–T_P^- can form a resonance system with the versatile oxygen–T_P plus carbon – P_N^* combination of the double-bonded oxygen. Finally, in phenols the OH-group is bound with its oxygen–D_N to a D_N of the benzene ring, after which the oxygen–T_P^- becomes part of the resonance system in alkaline solutions.

2.4.6 Molecules of oxygen with nitrogen (O with N). The colorless gas nitric oxide (NO) is a free radical compound disobeying the octet rule. It dimerizes only upon condensing to a liquid (−152 °C), but the association of the presumed N-radicals is weak and reversible and the N–N distance in crystalline NO (−164 °C) is reported to be nearly twice the NO distance.[65,66] In the new model, NO is a symmetrically balanced molecule containing a triple bond between oxygen and nitrogen with the oxygen atom containing the unpaired electron (Fig. 20).

The oxygen – $^3_2$He*-unit has formed a bridgehead with its D_N. The square proton of the $^3_2He_N^*$-unit has kept its non-activated low-energy electron, whereas the remaining D_N of the $^3_2He_N^*$-unit together with the D_N form two bonds with the hybridized nitrogen–($T_P + D_P$). The third bond is formed between the oxygen–T_P and the nitrogen–D_N. In the compound NO^+ the square $^3_2He_N^*$-proton has lost its electron.

In $NO_2^•$ and NO_2^+,[67] the nitrogen atom is the central atom with a bridge-headed ($^3_2He_N^* + D_N$)-unit and the square proton of the $^3_2He_N^*$-unit keeping its non-activated low energy electron or not. Each oxygen–T_P is bound to the D_N's of the bridge-headed ($^3_2He_N^* + D_N$)-unit, each oxygen–D_N is bound to the hybridized nitrogen–($T_P + D_P$).

A final illustrative example is the acid HNO_3. This acid is a well-known octet rule disobeying compound (formally N^{5+} surrounded by 10 electrons) for which a Lewis structure has been developed. In the new atom model, the two double bonded oxygen atoms are bound with their D_N to the hybridized nitrogen–($T_P + D_P$) of the nitrogen atom and with their T_P to the protons of the $^3_2He_N^*$-unit. The oxygen of the OH-group bears an H-atom at its T_P, and is bound with its D_N to the nitrogen–D_N (Fig. 20).

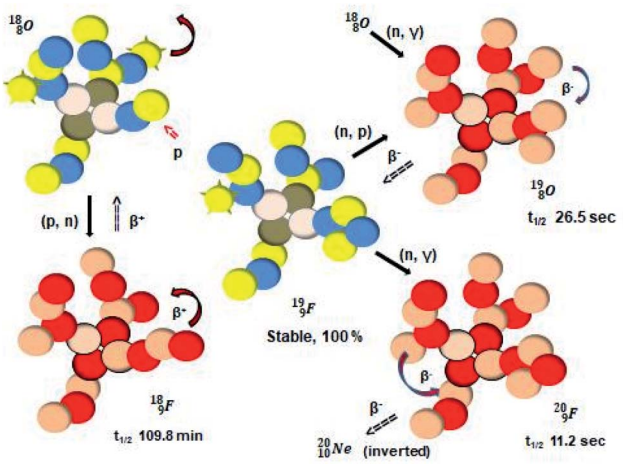

Fig. 21 Constellation of the main isotopes of fluorine ($1s^2 2s^2 2p^5$) in the new model, including illustrative conversions.

Open Access Article. Published on 19 August 2021. Downloaded on 2/7/2026 11:39:10 PM.
This article is licensed under a Creative Commons Attribution-NonCommercial 3.0 Unported Licence.

2.5 Fluorine ($Z = 9$), neon ($Z = 10$) and their lone pairs

2.5.1 Fluorine. The fluorine atom $^{19}_{9}$F (100% abundance) possesses an open $^{4}_{2}He^{*}_{N}$-unit and a closed $^{4}_{2}He_{N}$-unit at the anchor neutron side, and, like $^{16}_{8}$O, a T_P and an open neutron-deficient $^{4}_{2}He_{P}$-unit at the anchor proton side (Fig. 21).

Closure of the latter unit by a neighboring neutron from an H_2O or HF molecule gives rise to a hydrogen bond. With its $n = 4, p = 3$ at the anchor proton side and $n = 3\frac{1}{2}, p = 4$ at the anchor neutron side, $^{19}_{9}$F follows the stability rules.

Radioisotope $^{18}_{9}$F ($t_{1/2}$ 110 min.), a widely known component of PET-chemistry, lacks the square neutron in the $^{4}_{2}He^{*}_{N}$-unit at the anchor neutron side. It is produced by a (p, n) reaction on $^{18}_{8}$O:[68] the proton impact takes place at the D_N, forming a $^{3}_{2}He_{N}$-unit, and throws out the square neutron of the $^{5}_{2}He^{*}_{P}$-unit (last in, first out); $^{18}_{9}$F decays *via* β^+-emission back to $^{18}_{8}$O (Fig. 21). Notably, $^{18m}_{9}$F ($t_{1/2}$ 162 nanoseconds, decay to $^{18}_{9}$F[69]) is the result of the impact at D_N and throwing out the square neutron of the $^{4}_{2}He^{*}_{N}$-unit, giving two $^{3}_{2}He_{N}$-units with full energy protons; the IT to $^{18}_{9}$F implies the fast shift of a neutron from the $^{5}_{2}He_{P}$-unit to this very neutron-deficient anchor neutron side as a temporarily better situation. Radioisotope $^{20}_{9}$F, produced by a (n, γ) reaction on $^{19}_{9}$F[70] appears to be very instable ($t_{1/2}$ 11 s) with its $n = 4$, $p = 4$ at the anchor neutron side and its $n = 5$, $p = 3$ at the anchor proton side, and decays quickly to $^{20}_{10}$Ne Atom $^{17}_{9}$F ($t_{1/2}$ 65 s, produced by a (d, *n*) reaction on $^{16}_{8}$O[71]), bears two $^{3}_{2}He_{N}$-units and decays to $^{17}_{8}$O *via* β^+-emission (conversion of a proton from one of the $^{3}_{2}He_{N}$-units into a square neutron onto the other $^{3}_{2}He_{N}$-unit); $^{16}_{9}$F and lower are proton emitters.

2.5.2 Neon. With the noble gas neon, the quantum mechanical $2s^2,2p^6$-series ends. Its main isotope $^{20}_{10}$Ne (abundance 90.48%) possesses at the anchor proton side a closed $^{4}_{2}He_{P}$-unit and a $^{5}_{2}He_{P}$-unit, at the anchor neutron side a $^{3}_{2}He^{*}_{N}$-unit and a closed $^{4}_{2}He_{N}$-unit. The $^{5}_{2}$He- and $^{3}_{2}$He-units are hybridized, and so are both $^{4}_{2}$He-units (Fig. 22).

Fig. 22 also shows the constellation of the stable isotopes $^{21}_{10}$Ne (0.27% abundance) and $^{22}_{10}$Ne (abundance 9.25%), and of the instable $^{19}_{10}$Ne ($t_{1/2}$ 17.3 s). In the $^{21}_{20}$Ne atom, the $^{3}_{2}He^{*}_{N}$-unit has become a $^{4}_{2}He^{*}_{N}$-unit with a square neutron like in $^{19}_{9}$F. The $^{22}_{10}$Ne atom bears two $^{5}_{2}He_{P}$-units (one with a square neutron) at the anchor proton side, and two $^{4}_{2}He_{N}$-units at the anchor neutron side (one with a square neutron). Neon isotopes $^{20}_{10}$Ne, $^{21}_{10}$Ne both fit with the stability rules, with their $n = 5, p = 4$ at the anchor proton side and their $n = 3, p = 3\frac{1}{2}$ and $n = 3\frac{1}{2}, p = 4$, respectively, at the anchor neutron side. The $^{22}_{10}$Ne atom is stable with $n = 5\frac{1}{2}$, $p = 4$ at the anchor proton side, and is, therefore, the second isotope that follows the special $n = p + 1\frac{1}{2}$ anchor proton side stability rule. As was the case with $^{18}_{8}$O, the extra neutron appears to remain as a square neutron in the $^{4}_{2}He_{P}$ lone pair, as $^{5}_{2}He^{*}_{P}$-unit, because conversion of a neutron into a proton yielding $^{22}_{11}$Na, does not occur. Again it is the other way around: radioactive $^{22}_{11}$Na decays to $^{22}_{10}$Ne.

In the short-living radioisotope $^{19}_{10}$Ne, the $^{5}_{2}He_{P}$-unit at the anchor proton side is replaced by a $^{4}_{2}He_{P}$-unit. During its production *via* a (p, n) reaction on $^{19}_{9}$F,[72] proton impact takes place at the T_P of $^{19}_{9}$F while the square neutron of the $^{4}_{2}He^{*}_{N}$-unit is thrown out. Atom $^{19}_{10}$Ne decays back to $^{19}_{9}$F *via* conversion of a proton from one of the $^{4}_{2}He_{P}$-units into a square neutron onto the $^{3}_{2}He_{N}$-unit (β^+-emission). Radioisotope $^{18}_{10}$Ne ($t_{1/2}$ 1.7 s) bears two $^{4}_{2}He_{P}$-units at the anchor proton side, and two $^{3}_{2}He_{N}$-units at the anchor neutron side. It decays as a first step to instable $^{18}_{9}$F by conversion of a proton of one of the $^{4}_{2}He_{P}$-units below into a neutron at one of the $^{3}_{2}He_{N}$-units above. The short-living radioisotopes $^{23}_{10}$Ne ($t_{1/2}$ 37.1 s), and $^{24}_{10}$Ne ($t_{1/2}$ 3.38 min) at the right side of $^{22}_{10}$Ne will be dealt with in a forthcoming paper.

So in the new model also the last two elements of the $2s^2,2p^6$-series, fluorine and neon, follow the remarkable regularity and consistency with respect to the stability or instability of the atoms. All stable isotopes $Z = 3$–10 appear to follow a strict $n = p - \frac{1}{2}$ pattern at the anchor neutron side, and a $n = p + 1$ pattern at the anchor proton side; only for $^{18}_{8}$O and $^{22}_{10}$Ne the pattern is $n = p + 1\frac{1}{2}$. Any deviation from these patterns leads to conversion. Another regularity is that the EC-decay of radioisotope $^{7}_{4}$Be as well as the β^+-decay of the nuclear medicine PET-isotopes $^{11}_{6}$C, $^{13}_{7}$N, $^{15}_{8}$O and $^{18}_{9}$F and of radioisotopes $^{17}_{9}$F, $^{19}_{10}$Ne all imply conversion of a full energy proton into a square neutron. Even for $^{10}_{6}$C and $^{14}_{8}$O this is the case, although they seem to look like an exception: the newborn square neutron, temporarily bound as a square neutron to both P_N's at the anchor neutron side, exchanges energy with the neighboring proton, leaving a P^{*}_{N} or $^{3}_{2}He^{*}_{N}$, respectively, behind under formation of a D_N.

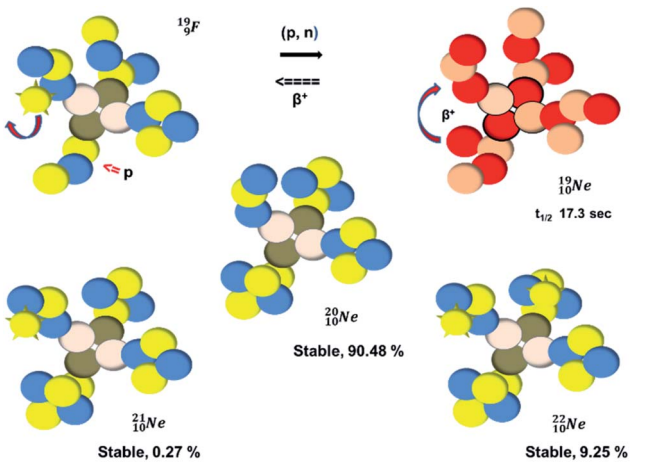

Fig. 22 Constellation of the main isotopes of neon ($1s^2 2s^2 2p^6$) in the new model, including one illustrative conversion.

2.5.3 Poor fluorine atom. The molecule F_2 is extremely reactive with high heat release, and its bond strength is rather substandard (33 kcal mole^{-1}).[73] Taking $^{20}_{10}$Ne, $^{21}_{10}$Ne and $^{22}_{10}$Ne as model, it can be derived that covalent bond formation strives in average for a chemical "$^{4}_{2}$He to $^{5}_{2}$He-unit" formation at the anchor proton side, and a chemical "$^{3}_{2}$He to $^{4}_{2}$He-unit" formation at the neutron anchor side. From the fact that F possesses a T_P as chemical binding unit, it follows that in case of the F_2 molecule a T_P with a T_P is a very poor bond-proposition, because it would lead to a chemical "$^{6}_{2}$He-unit" as covalent bond. To avoid formation of an unfavorable chemical $^{6}_{2}$He-unit as covalent bond, the T_P of the F atom is compelled to hybridize with its $^{4}_{2}He_{P}$-unit. This forces the anchor protons a little closer to each other (and so the anchor neutrons a little further away from

© 2021 The Author(s). Published by the Royal Society of Chemistry

Open Access Article. Published on 19 August 2021. Downloaded on 2/7/2026 11:39:10 PM.
This article is licensed under a Creative Commons Attribution-NonCommercial 3.0 Unported Licence.

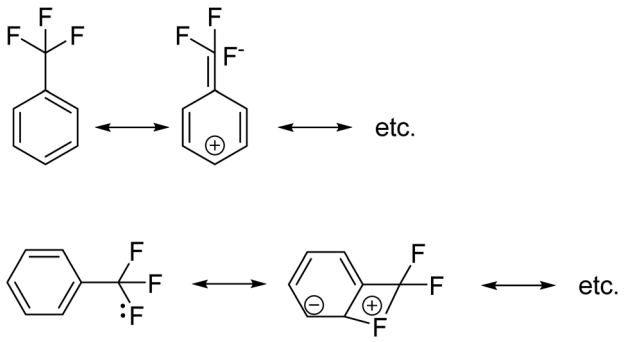

Fig. 23 CF_3–C_6H_5 in its double-bond no-bond resonance hypothesis (positive hyperconjugation hypothesis) and in its negative hyperconjugation hypothesis.

each other) creating an energetically disadvantageous tension. The high heat release upon reaction therefore originates from restoring the "normal" distance between the anchor protons and anchor neutrons. For the O_2 molecule this bonding aspect is less problematic. The O_2 molecule contains a solid bond between both D_N's and a more fragile bond between both T_P's, the neutrons of which are hybridized with their ${}^3_2He^*_N$-units, so no "${}^6_2$He-ish" covalent bond, and therefore O_2 reacts less extreme. The same holds for hydrogen peroxide (H_2O_2) and its T_P–T_P bond. In acetyl hypofluorite (CH_3COOF), the F-atom is bound to the T_P of the oxygen atom which is hybridized with its ${}^3_2He^*_N$-unit, and therefore this F-atom reacts less vigorous than in F_2 (approximately as vigorous as H_2O_2).

Upon reaction with the carbon atom, the fact that the T_P of fluorine strongly prefers covalent "${}^5_2$He"-bond formation leads to subtle conflicts. Upon bond formation with the D_P of carbon, the hybridized neutron (from D_N or T_P) has to be pushed aside. This forced re-hybridization will have its effect on the carbon skeleton. At the anchor neutron side of the carbon atom, bond formation with D_N seems fine for the T_P of F, but a "${}^5_2$He"-bond is too much for the carbon–D_N. The compromise will be a sort of "${}^{4.5}_2$He"-bond with the hybridized (P_N + D_N)-units. Bond formation with hybridized P_N will in case of a mono-fluorinated aliphatic compound suffer from easy elimination of HF in a process that resembles the keto–enol tautomerism for a carbonyl group. Finally, in the CF_3-group (one F at the D_P and two F's at the hybridized $P_N + D_N$), the T_P of the carbon atom has become fully isolated and therefore exhibits more or less the same chemical behavior as the T_P of F, which explains *e.g.* the chemistry of the CF_3-group in trifluorotoluene (CF_3–C_6H_5): in CF_3–C_6H_5, the isolated T_P of the carbon atom of the CF_3-group, bound at the D_P of the benzene ring, forces the benzene ring to re-hybridize, while the open neutron-deficient ${}^4_2He_P$-unit of the fluorine atoms of the CF_3-group interacts with the D_N-neutron of the neighboring carbon atoms of the benzene ring (the *ortho* positions). Notably, this explanation according to the new atom model, compiles in an elegant way the 'double-bond no-bond' resonance hypothesis, and the hypothesis wherein one of the three F-atoms of the CF_3-group has formed a bond with one of the carbon atoms at the *ortho*-position of the benzene ring (so with F^+ formation) (Fig. 23).[74,75]

3 Concluding remarks

This paper describes a revolutionary adjustment of the reigning quantum mechanical atom model for the elements with $Z = 1$–10. The new atom model is based on the premise that in elements with low Z the mass is not concentrated for 99.9% in a very small dense positive inner core. In the adjusted model, which comprised a ${}^4_2$He-unit as backbone with various subunits (P_N, D_N, D_P, T_P, ${}^3_2He_N$, ${}^4_2He_N$, ${}^4_2He_P$ and ${}^5_2He_P$), the neutron has been given a much more prominent role than it has in the reigning quantum mechanical model. It is not just there to assist the strong force to surpass the repulsive coulombic forces between the protons in the nucleus, but the neutron is the modus operandi of the hybridization principle, molecular geometry and hydrogen bonds, and as such plays a part in chemical reactivity, bond length and bond strength, as shown for F_2. Moreover, the neutron plays an important role in the subtle change in the hybridization in the atom constellations of the molecule upon phase transition, as displayed for the boiling H_2O molecule.

The atom constellations arising from this new model not only provide an answer to the re-hybridizing power of fluorine, our primary objective. They also appear to be perfectly in accordance with the linear molecular geometry of beryllium, the trigonal planar molecular geometry of boron, and the tetrahedral molecular geometry of carbon, nitrogen and oxygen (including the special lone pairs of the latter two). In addition, the derived atom constellations follow a consistent pattern with respect to the stability of isotopes, the produced radioisotopes thereof, and the respective decay modes of the latter.

Other key topics are the new sound basis for covalent bond formation (formation of a "chemical" He-unit between a P_N, D_N, D_P or T_P-subunit with one of the subunits of the other atom), and the re-definition of the hydrogen bond (neutron bond between the T_P-subunit of the atom and the neutron-deficient ${}^4_2He_P$-unit or ${}^3_2He^*_N$-unit of a neighboring molecule). Furthermore, the new model offers an improved answer to phenomena like the hybridization principle, inversion, chirality, resonance and the secret behind the chemical reactivity of the empty orbital of boron.

In a forthcoming "Part II" we will investigate whether the adjusted model still holds for the slightly heavier elements $Z =$ 11–20, and if so, what the configurations of the atoms Na ($Z =$ 11) through Ca ($Z = 20$) look like in the new approach. And, as a further matter, whether the new model can provide a genuine solution for the occurrence of multiple valencies of the elements P, S, and Cl, with special attention to the well-known "octet-rule violating" compounds H_3PO_4, H_2SO_4 and $HClO_4$.

Conflicts of interest

Prof. Dr A. D. Windhorst is editor-in-chief of Nuclear Medicine & Biology.

Note added after first publication

This article replaces the version published on 19th August 2021, which contained multiple formatting errors.

Open Access Article. Published on 19 August 2021. Downloaded on 2/7/2026 11:39:10 PM.
This article is licensed under a Creative Commons Attribution-NonCommercial 3.0 Unported Licence.

References

1 J. J. Thomson, *Phil. Mag. Ser.*, 1904, **7**(39), 237.
2 K. Lord, *Phil. Mag. Ser.*, 1902, **3**(15), 257.
3 E. Rutherford, *Phil. Mag. Ser.*, 1911, **6**(21), 669.
4 N. Bohr, *Phil. Mag. Ser.*, 1913, **26**(151), 1.
5 E. Schrodinger, *Ann. Phys.*, 1926, **384**(4), 273.
6 W. Heisenberg, *Z. Phys.*, 1927, **43**(3–4), 172.
7 L. Pauling, *J. Am. Chem. Soc.*, 1931, **53**(4), 1367.
8 M. D. Harmony, *Chem. Soc. Rev.*, 1972, **1**, 211.
9 X.-Z. Li, B. Walker and A. Michaelides, *Proc. Natl. Acad. Sci. U. S. A.*, 2011, **108**(16), 6369.
10 G. N. Lewis, *J. Am. Chem. Soc.*, 1916, **38**, 762.
11 J. F. Ogilvie, *J. Chem. Educ.*, 1990, **67**(4), 280.
12 R. D. Chambers, *Fluorine in Organic Chemistry*, Wiley-Interscience, John Wiley & Sons, 1973.
13 J. Hine, *J. Am. Chem. Soc.*, 1963, **85**(20), 3239.
14 P. Politzer and J. W. Timberlake, *J. Org. Chem.*, 1972, **37**(22), 3557.
15 G. W. M. Visser, *Trends Org. Chem.*, 1993, **4**, 379.
16 G. W. M. Visser and J. D. M. Herscheid, *14th Intern. Symp. on Fluorine Chem.*, 1994, Yokohama, Japan. https://www.researchgate.net/publication/292605267_The_s-orbital_character_deficiency_of_fluorine_as_driving_force_to_react_with_organic_substrates.
17 G. W. M. Visser, *11th Eur. Symp. on Fluorine Chem.*, 1995, Bled, Slovenia. https://www.researchgate.net/publication/295860798_On_the_Chemical_Behaviour_of_Fluorine_The_Unusual_and_Unexpected_made_usual_11th_European_Symposium_on_Fluorine_Chemistry_Bled_1995.
18 H. A. Bent, *Chem. Rev.*, 1961, **61**(3), 275.
19 A. D. Windhorst, H. Timmerman, E. A. Worthington, G. J. Bijloo, P. H. J. Nederkoorn, W. M. P. B. Menge, R. Leurs and J. D. M. Herscheid, *J. Med. Chem.*, 2000, **43**, 1754.
20 G. W. M. Visser, R. P. Klok and A. D. Windhorst, *15th Intern. Symp. on Fluorine Chem.*, 1997, Vancouver, Canada, https://www.researchgate.net/publication/295860864_Fluorine_and_the_Problem_with_Electrostatic_Effects_15th_International_Symposium_on_Fluorine_Chemistry_Vancouver_August_2-7_1997.
21 G. Portalone, G. Schultz, A. Domenicano and I. Hargittai, *J. Mol. Struct.*, 1984, **118**(1–2), 53.
22 *Radionuclide Transformations – Energy and Intensity of Emissions, Radiation Protection*, ICRP PUBLICATION 38, Pergamon Press Ltd., Headington Hill Hall, Oxford, England, 1983.
23 H. H. Voge, *J. Chem. Phys.*, 1948, **16**, 984.
24 E. Hückel, *Z. Phys.*, 1930, **60**(7–8), 423.
25 W. E. Palke, *J. Am. Chem. Soc.*, 1986, **108**(21), 6543.
26 P. A. Schultz and R. P. Messmer, *J. Am. Chem. Soc.*, 1993, **115**(21), 10925.
27 K. B. Wiberg, *Acc. Chem. Res.*, 1996, **29**(5), 229.
28 P. Maitland and W. H. Mills, *Nature*, 1935, **135**, 994.
29 (*a*) F. A. Kekulé, *Ann. Chem. Pharm.*, 1886, **137**(2), 129; (*b*) A. Ladenburg, *Ber. Dtsch. Chem. Ges.*, 1869, **2**, 140.
30 Y. Liu, P. Kilby, T. J. Frankcombe and T. W. Schmidt, *Nat. Commun.*, 2020, **11**, 1210.
31 R. D. O'Neal and M. Goldhaber, *Phys. Rev.*, 1940, **58**, 574.
32 W. L. Imhof, R. G. Johnson, F. J. Vaughn and M. Walt, *Phys. Rev.*, 1959, **114**, 1037.
33 (*a*) H. R. Crane, L. A. Delsasso, W. A. Fowler and C. C. Lauritsen, *Phys. Rev.*, 1935, **47**, 971; (*b*) L. A. Delsasso, W. A. Fowler and C. C. Lauritsen, *Phys. Rev.*, 1935, **48**, 848; (*c*) D. S. Bayley and H. R. Crane, *Phys. Rev.*, 1937, **52**, 604.
34 (*a*) K. Arai, D. Baye and P. Descouvemont, *Nucl. Phys. A*, 2002, **699**(3), 963; (*b*) J. J. He, S. Z. Chen, C. E. Rolfs, S. W. Xu, J. Hu, X. W. Ma, M. Wiescher, R. J. deBoer, T. Kajino, M. Kusakabe, L. Y. Zhang, S. Q. Hou, X. Q. Yu, N. T. Zhang, G. Lian, Y. H. Zhang, X. H. Zhou, H. S. Xu and W. L. Zhan, *Phys. Lett. B*, 2013, **725**, 287.
35 T. Kobayashi, G. Bengua, K. Tanaka and Y. Nakagawa, *Phys. Med. Biol.*, 2007, **52**, 645.
36 L. H. Rumbaugh, R. B. Roberts and L. R. Hafstad, *Phys. Rev.*, 1938, **54**, 657.
37 (*a*) D. J Hughes, C. Eggler and C. M. Huddleston, *Phys. Rev.*, 1947, **71**, 26; (*b*) D. J. Hughes, C. Eggler and B. E. Alburger, *Phys. Rev.*, 1950, **77**, 726.
38 J. Chadwick, *Proc. R. Soc. A*, 1932, **136**(830), 692.
39 (*a*) R. Sherr, H. R. Muether and M. G. White, *Phys. Rev.*, 1948, **74**, 1239; (*b*) R. Sherr, H. R. Muether and M. G. White, *Phys. Rev.*, 1949, **75**, 282.
40 W. H. Barkas, *Phys. Rev.*, 1939, **56**, 287.
41 (*a*) H. R. Crane, L. A. Delsasso, W. A. Fowler and C. C. Lauritsen, *Phys. Rev.*, 1935, **47**, 887; (*b*) W. A. Fowler, L. A. Delsasso and C. C. Lauritsen, *Phys. Rev.*, 1936, **49**, 561.
42 S. Neelam and R. Chatterjee, *Phys. Rev. C*, 2015, **92**, 044615.
43 J. M. Freeman and R. C. Hanna, *Nucl. Phys.*, 1957, **4**, 599.
44 (*a*) W. Y. Chang, M. Goldhaber and R. Sagane, *Nature*, 1937, **139**, 962; (*b*) J. K. Bienlein and E. Kalsch, *Nucl. Phys.*, 1964, **50**, 202.
45 I. Curie and F. Joliot, *Compt. Rend.*, 1934, **198**, 254.
46 C. D. Ellis and W. J. Henderson, *Nature*, 1935, **135**, 429.
47 L. N. Ridenour and W. J. Henderson, *Phys. Rev.*, 1937, **52**, 889.
48 R. N. Hall and W. A. Fowler, The Cross Section for the Radiative Capture of Protons by C-12 near 100 keV, *Phys. Rev.*, 1950, **77**, 197.
49 W. A. S. Lamb and R. E. Hester, *Phys. Rev.*, 1957, **107**, 550.
50 D. M. Yost, L. N. Ridenour and K. Shinohara, *J. Chem. Phys.*, 1935, **3**, 133.
51 (*a*) R. E. Adamson, Jr, W. W. Buechner, W. M. Preston, C. Goodman and D. M. Van Patter, *Phys. Rev.*, 1950, **80**, 985; (*b*) S. W. Kitwanga, P. Leleux, P. Lipnik and J. Vanhorenbeeck, *Phys. Rev. C*, 1989, **40**, 35.
52 V. A. Muminov, S. Mukhamedov, B. Sultanov and T. Khamrakulov, *Izv. Akad. Nauk Uzb. SSR, Ser. Fiz.-Mat. Nauk*, 1974, **1**, 56.
53 S. Ruben and M. D. Kamen, *Phys. Rev.*, 1941, **59**, 349.
54 W. H. Barkas, *Phys. Rev.*, 1939, **56**, 287.
55 Y. Suleymanov, *Science*, 2019, **366**(6471), 1325.

© 2021 The Author(s). Published by the Royal Society of Chemistry

Open Access Article. Published on 19 August 2021. Downloaded on 2/7/2026 11:39:10 PM.
This article is licensed under a Creative Commons Attribution-NonCommercial 3.0 Unported Licence.

56 N. V. Cohan and C. A. Coulson, *Trans. Faraday Soc.*, 1956, **52**, 1163.
57 K. Abbaspour Tehrani and N. de Kimpe, *Sci. Synth.*, 2004, **27**, 245.
58 M. Raban, *J. Chem. Soc. D*, 1970, 1415–1416.
59 G. J. Karabatsos and S. S. Lande, *Tetrahedron*, 1968, **34**(10), 3907.
60 L. Seren, W. E. Moyer and W. Sturm, *Phys. Rev.*, 1946, **70**, 561.
61 D. E. Alburger, A. Gallman and D. H. Wilkinson, *Phys. Rev.*, 1959, **116**, 939.
62 E. B. Paul and R. L. Clark, *Can. J. Phys.*, 1953, **31**, 267.
63 A. R. Barnett, *Nucl. Phys. A*, 1968, **120**, 342.
64 (*a*) M. Laing, *J. Chem. Educ.*, 1987, **64**, 124; (*b*) M. Ceriotti, W. Fang, P. G. Kusalik, R. H. McKenzie, A. Michaelides, M. A. Morales and T. E. Markland, *Chem. Rev.*, 2016, **116**, 7529.
65 S. G. Kukolich, *J. Am. Chem. Soc.*, 1982, **104**, 4715.
66 N. N. Greenwood and A. Earnshaw, *Chemistry of the Elements*, Butterworth-Heinemann, 2nd edn, 1997.
67 H. A. Bent, *Inorg. Chem.*, 1963, **2**, 747.
68 L. A. DuBridge, S. W. Barnes, J. H. Buck and C. V. Strain, *Phys. Rev.*, 1938, **53**, 447.
69 F. D. Becchetti, J. A. Brown, K. Ashktorab, J. W. Jänecke, W. Z. Liu, D. A. Roberts, R. J. Smith, J. J. Kolata, K. Larrikin, A. Morsad and R. E. Warner, *Nucl. Instrum. Methods Phys. Res., Sect. B*, 1991, **56–57**(part 1), 554.
70 (*a*) S. S. Glickstein and R. G. Winter, *Phys. Rev.*, 1963, **130**, 1281; (*b*) P. Spilling, H. Gruppelaar, H. F. de Vries and A. M. J. Spits, *Nucl. Phys. A*, 1968, **113**, 395.
71 (*a*) H. W. Newson, *Phys. Rev.*, 1935, **48**, 790; (*b*) V. Perez-Mendez and P. Lindenfield, *Phys. Rev.*, 1950, **80**, 1097.
72 (*a*) M. G. White, L. A. Delsasso, J. G. Fox and E. C. Creutz, *Phys. Rev.*, 1939, **56**, 512–518; (*b*) G. Schrank and J. R. Richardson, *Phys. Rev.*, 1952, **86**, 248.
73 L. E. Forslund and N. Kaltsoyannis, *New J. Chem.*, 2003, **27**, 1108.
74 J. D. Roberts, R. L. Webb and E. A. McElhill, *J. Am. Chem. Soc.*, 1950, **72**(1), 408.
75 D. Holtz, *Chem. Rev.*, 1971, **71**, 139.

© 2021 The Author(s). Published by the Royal Society of Chemistry